Inferring the differences in incubation-period and generation-interval distributions of the Delta and Omicron variants of SARS-CoV-2

Abstract

Estimating the differences in the incubation-period, serial-interval, and generation-interval distributions of SARS-CoV-2 variants is critical to understanding their transmission dynamics and outbreak control. However, the impact of epidemic dynamics is often neglected in estimating the timing of infection and transmission—for example, when an epidemic is growing exponentially, a cohort of infected individuals who developed symptoms at the same time are more likely to have been infected recently. Here, we re-analyze incubation-period and serial-interval data describing transmissions of the Delta and Omicron variants from Netherlands at the end of December 2021. Previous analysis of the same data set reported shorter mean observed incubation period (3.2 days vs 4.4 days) and serial interval (3.5 days vs 4.1 days) for the Omicron variant, but the number of infections caused by the Delta variant decreased during this period as the number of Omicron infections increased. When we account for growth-rate differences of two variants during the study period, we estimate similar mean incubation periods (3.8–4.5 days) for both variants but a shorter mean generation interval for the Omicron variant (3.0 days; 95% CI: 2.7–3.2 days) than for the Delta variant (3.8 days; 95% CI: 3.7–4.0 days). The differences in realized generation intervals may be driven by the network effect—higher effective reproduction numbers of the Omicron variant can cause faster susceptible depletion among contact networks, which in turn prevents late transmission (and therefore shortening realized generation intervals). Using up-to-date generation-interval distributions is critical to accurately estimating the reproduction advantage of the Omicron variant.

1 Introduction

Estimating transmission advantages of new SARS-CoV-2 variants is critical to predicting and controlling the course of the COVID-19 pandemic [1]. Transmission advantages of invading variants are typically characterized by the ratios of reproduction numbers, $\mathcal{R}_{\text{inv}}/\mathcal{R}_{\text{res}}$, and the differences in growth rates, $r_{\text{inv}} - r_{\text{res}}$. These two quantities are linked by the generation-interval distributions of the resident and invading variants. For example, an invading variant with shorter generation intervals—defined as the time between infection of the infector and the infectee—will exhibit faster epidemic growth ($r_{\text{inv}} > r_{\text{res}} > 0$) even if their reproduction numbers are identical ($\mathcal{R}_{\text{inv}} = \mathcal{R}_{\text{res}} > 1$).

Estimating the generation-interval distribution is challenging, in part due to difficulties in observing actual infection events. Many researchers primarily focus on comparisons of other transmission intervals, such as the time between symptom onsets (also referred to as serial intervals) or between testing events [2] of the infector and the infectee. Each of these transmission-interval distributions are subject to dynamical effects, which can cause transmission-interval distributions to systematically differ from the corresponding generation-interval distribution. For example, when the epidemic is growing, there will be more recent infections. Therefore, we are more likely to observe recently infected individuals among a cohort of infectors who developed symptoms at the same—we refer to this effect as the "dynamical bias". In this case, their incubation periods will be shorter, on average, than those of their infectees, causing the mean serial interval to be longer than the mean generation interval [3]. Therefore, observed differences in transmission-interval distributions between variants are not necessarily equivalent to differences in the underlying generation-interval distributions, especially if their growth rates differ.

Here, we re-analyze serial-interval data collected by [4], representing within- and between-household transmissions of the Delta and Omicron variants from the Netherlands between 13 and 26 December 2021. The study found shorter mean serial intervals (3.5 vs 4.1 days) and mean incubation periods (3.2 vs 4.4 days) for transmission pairs with S-gene target failure (mostly Omicron during the study period) than without (mostly Delta), but did not consider dynamical biases caused by growth-rate differences in their inference: during this period, the Omicron cases were increasing, whereas the Delta cases were decreasing. Here, we take the epidemiological context in the Netherlands during the study period into account to provide corrected estimates for the incubation periods and generation-interval distributions of the Delta and Omicron variants. We show that using up-to-date generation-interval distributions is critical to accurately estimating the reproduction advantage (i.e., the ratio between the reproduction numbers of the invading and resident variants) of emerging SARS-CoV-2 variants.

2 Methods

2.1 Data

We analyze time series of reported COVID-19 cases (`https://data.rivm.nl/covid-19/`) and proportions of SARS-CoV-2 variants detected (`https://www.rivm.nl/coronavirus-covid-19/virus/varianten`) from the Netherlands between 29 November 2021 and 30 January 2022. Data sets are publicly available on the National Institute for Public Health and the Environment (RIVM) website.

Serial interval data are taken from [4]. Infector-infectee pairs were identified through contact tracing, and their symptom onset dates were reported through a national surveillance database. Serial intervals were then calculated by taking the difference between symptom onset dates of the infector and the infectee. In order to ensure independence between serial intervals, one infectee was chosen at random for each infector in the original analysis. See original article for additional details of data collection.

Publicly available data are aggregated by the length of the serial interval in days and do not include additional individual-level information, such as exposure dates or symptom onset dates. The data consists of 2529 transmission pairs and are further stratified by the presence of S gene target failure (SGTF), week of infectors' symptom onset date (week 50, 13–19 December 2021, and week 51, 20–26 December 2021), and the type of transmission (within or between households). In the main text, we combine data from weeks 50 and 51 of 2021 (13–26 December) and present a stratified analysis in Supplementary Material. For simplicity, we refer to transmission pairs with and without SGTFs as Omicron and Delta transmission pairs, respectively. Incubation period data are not publicly available with the original article; instead, we rely on previous estimates [4] to derive growth-rate-adjusted incubation-period distributions.

2.2 Estimating epidemic growth rates

In order to accurately estimate incubation-period and generation-interval distributions of the Delta and Omicron variants, we have to take their epidemiological dynamics—in particular, the differences in their growth rates—into account. To estimate the growth rates differences of the Delta and Omicron variants, we first estimate the number of COVID-19 cases caused by each variant by multiplying reported weekly numbers of cases by the proportion of Delta and Omicron variants detected—we use weekly time series to smooth over patterns of testing and reporting within each week. We note that the proportion of Delta and Omicron variants detected is reported by the date of sampling, whereas the case data are reported by the date of reports, meaning that there is some delay between the two data. For simplicity, we do not account for this delay, which in turn affects our growth-rate estimates; instead, we later perform sensitivity analysis to assess how growth rates

affect the inferences of the incubation-period and generation-interval distributions. We also do not account for uncertainties around the estimates of the proportion of each variant—almost 2000 samples were tested on each week between the week of November 28, 2021, and the week of January 23, 2022, making the uncertainty negligible.

We then fit a generalized additive model [5] to to the logged weekly case estimates to obtain smooth trajectories for case time series. More specifically, we model the logged weekly numbers of cases caused by each variant as a function of time using a shrinkage version of a cubic spline with restricted maximum likelihood (specified as `s(time, bs="cs")` using the `MGCV` package). We also assume normally distributed errors around the logged weekly cases. In principle, using negative-binomial likelihoods with a log link function is more appropriate for modeling count data, especially when data are overdispersed [6]; here, we use Gaussian likelihoods on logged cases because the inferred numbers of cases caused by each variant are not counts. Finally, we take the derivative of the predicted logged numbers of cases caused by each variant to obtain time-varying growth rate estimates.

To obtain confidence intervals on the estimated time-varying growth rates, we generate 1000 parameter sets by resampling spline coefficients from a multivariate normal distribution using the estimated variance-covariance matrices. We calculate time-varying growth rates from each parameter set and use equi-tailed quantiles to generate 95% confidence limits.

2.3 Estimating forward incubation-period distributions from backward incubation-period distributions

The incubation-period distributions from 513 individuals (258 Omicron and 255 Delta cases), with symptom onsets between 1 December 2021 and 2 January 2022, were previously reported in [4]. [4] used the methods of [7], which estimates incubation period by inferring distributions of time of infection for each individual from their known exposure dates. In particular, the methods of [7] assume that the infection time is uniformly distributed across exposure dates and compares the inferred infection time to a known symptom-onset time to calculate the incubation period for each individual. While this method may accurately estimate the infection time, and therefore the incubation period, of each individual, dynamical biases can still affect the distribution of the inferred incubation periods from this cohort.

More specifically, incubation periods (and other epidemiological delays) can be measured in two ways: forward and backward [3]. The forward incubation periods are measured from a cohort of individuals who were infected at the same time. We expect this forward incubation-period distribution $f_I(\tau)$ to remain relatively constant over the course of an epidemic of one given variant, although biases can arise in *observing* incubation periods, based on public or medical awareness of the disease. Backward incubation periods are measured from a cohort of individuals who developed symptoms at the same time. The backward incubation-period distribution

is sensitive to epidemic dynamics: the difference between the forward and backward distribution arises because forward incubation periods look forward from the reference point towards symptom development, which is an individual-level process, while backward incubation periods look backwards towards an infection event, which requires an interaction with an infectious individual.

In particular, when incidence of infection is growing exponentially, we are more likely to observe backward incubation periods that are shorter than the corresponding forward incubation periods because there will be relatively more individuals who were infected recently. Assuming that incidence of infection is changing exponentially at a constant rate r across the study period, the backward incubation-period distribution $b_I(\tau)$ corresponds to:

$$b_I(\tau) = \frac{\exp(-r\tau) f_I(\tau)}{\int_0^\infty \exp(-rx) f_I(x)\,\mathrm{d}x}. \tag{1}$$

Therefore, the backward incubation-period distribution $b_I(\tau)$ gives a biased estimate of the corresponding forward distribution $f_I(\tau)$. The method of [7] starts from observed symptom onsets, and estimates the backward incubation-period distribution.

Assuming a constant growth rate r, the corresponding forward incubation-period distributions can be calculated by inverting Eq. (1), taking into account that f_I is a probability distribution and therefore needs to be normalised to integrate to 1:

$$f_I(\tau) = \frac{\exp(r\tau) b_I(\tau)}{\int_0^\infty \exp(rx) b_I(x)\,\mathrm{d}x}. \tag{2}$$

Since incubation-period data are not provided, we are not able to fit Eq. (2) directly; instead we take the backward incubation-period distributions $b_I(x)$ estimated by [4], which was originally assumed to follow a Weibull distribution, and apply Eq. (2). In particular, [4] estimated the scale and shape parameters of the Weibull distribution to be 4.93 (95% CI: 4.51–5.37) and 1.83 (95% CI: 1.59–2.08), respectively, for the Delta cases, and 3.60 (95% CI: 3.23–3.98) and 1.50 ((95% CI: 1.32–1.70), respectively, for Omicron cases.

We also model the backward incubation-period distribution $b_I(\tau)$ using a Weibull distribution based on the assumptions of [4]. To account for uncertainties in the original parameter estimates, we rely on a sampling scheme, similar to the one we used for the growth rate analysis (in Section 2.2). First, we approximate the previously inferred posterior distributions of the shape and scale parameters of the Weibull distribution using a lognormal distribution—we parameterize the lognormal distribution such that (i) its median matches the median of the posterior distributions and (ii) the probability that a random variable following the specified lognormal distribution falls between the lower and upper credible limits is 95% [8]. We draw 1000 samples of the shape and scale parameters (for the backward distribution $b_I(\tau)$) from the specified lognormal distributions and estimate the corresponding forward distribution using Eq. (2). We take 95% equi-tailed quantiles to obtain 95% confidence intervals. We repeat the analysis across plausible ranges of r for the Delta and Omicron variants separately (discussed later).

2.4 Estimating forward generation-interval distributions from forward serial-interval distributions

Dynamical biases in the serial-interval distributions are more complex because the serial interval depends on the incubation periods of the infector and the infectee as well as the generation interval between them (Fig. 1). For example, [4] measured the forward serial-interval distributions from cohorts of infectors who developed symptoms during the same week. In this case, the forward serial interval τ_s can be expressed in the form [3]:

$$\tau_s = -\tau_{i,1} + \tau_{g,\text{symp}} + \tau_{i,2}, \tag{3}$$

where $\tau_{i,1}$ represents the backward incubation period of the infector (because all infectors developed symptoms at the same time), and $\tau_{i,2}$, represents the forward incubation period of the infectee. Here, $\tau_{g,\text{symp}}$ represents the generation interval between the infector and the infectee; we use the subscript symp to indicate that these generation intervals are measured from infectors who developed symptoms at the same time.

The generation-interval distribution for a symptom-based cohort ($\tau_{g,\text{symp}}$ in Eq. (3)) is biased (compared to the generation-interval distribution for an infection-based cohort) because infectors who developed symptoms at the same time will have shorter incubation periods (when the epidemic is growing) and therefore transmit earlier (Fig. 1A). This generation-interval distribution for a symptom-based cohort depends on the backward incubation-period distribution:

$$f_{G,\text{symptom}}(\tau) = \int_0^\infty f_{G|I}(\tau|x) b_I(x)\,\mathrm{d}x, \tag{4}$$

where $f_{G|I}(\tau|x)$ represents the forward generation-interval distribution conditional on a known value of the incubation period, x, and $b_I(x)$ represents the backward incubation-period distribution. Instead, the forward generation-interval distribution measured from a cohort of individuals who were infected at the time is expected to provide reliable estimates of the distribution across individuals (because their incubation-period distribution is expected to remain constant over time, Fig. 1B):

$$f_{G,\text{inf}}(\tau) = \int_0^\infty f_{G|I}(\tau|x) f_I(x)\,\mathrm{d}x. \tag{5}$$

Previous analyses of serial-interval distributions typically assumed that the incubation periods and generation intervals are independent [9]; in this case, the generation-interval distribution for the symptom-based and infection-based cohorts are identical.

When an epidemic is growing exponentially, there are two opposing effects affecting the relationship between the mean serial and generation interval. First, infectors in a given cohort are more likely to have shorter incubation periods than their infectees on average, $\mathbb{E}[\tau_{i,1}] < \mathbb{E}[\tau_{i,2}]$, causing the mean forward serial interval to be longer than the mean symptom-based generation interval ($\mathbb{E}[\tau_s] > \mathbb{E}[\tau_{g,\text{symp}}]$). Second, the mean symptom-based generation interval will be shorter than the mean

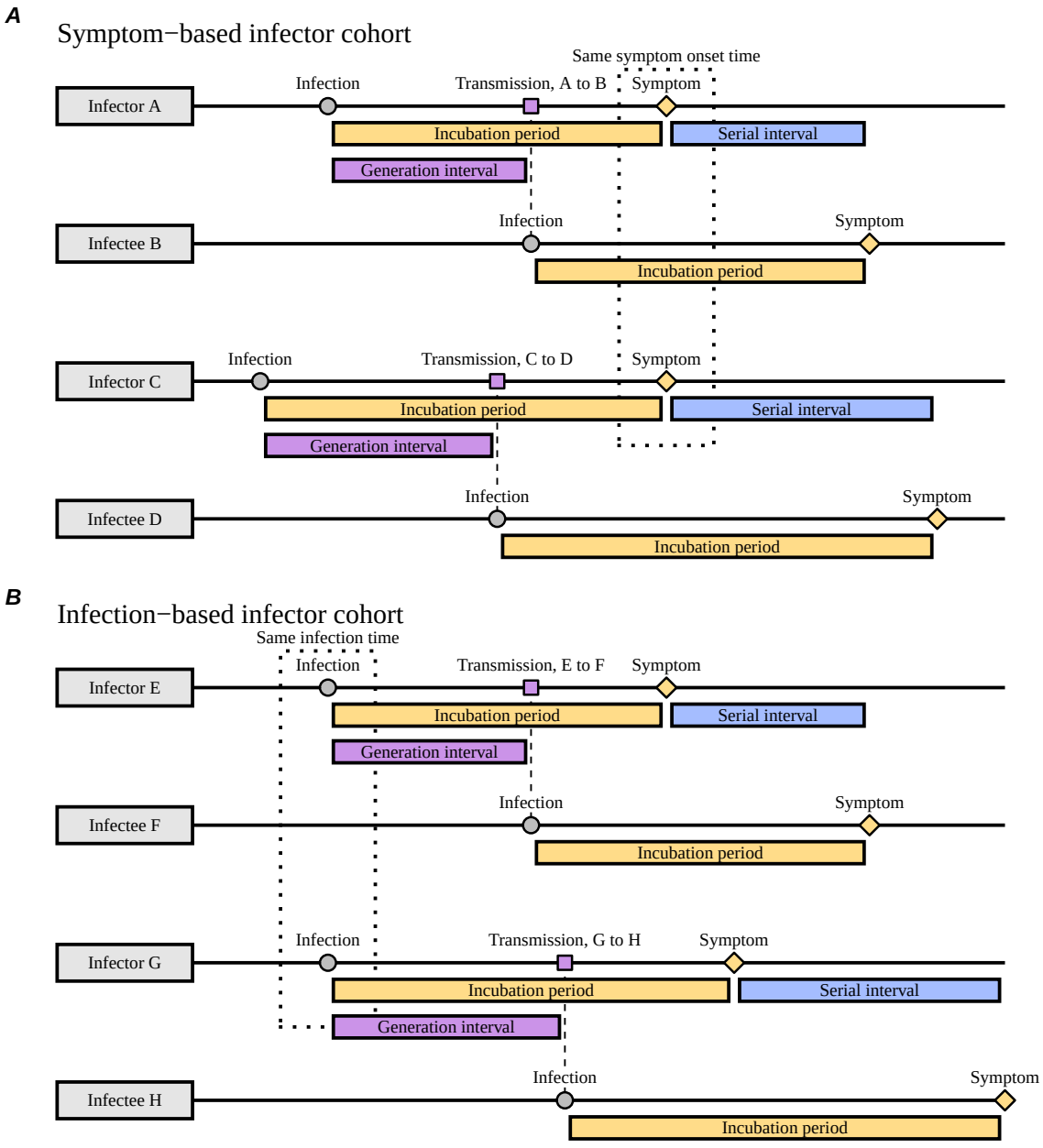

Figure 1: **Schematic diagrams of serial and generation intervals from symptom- and infection-based infector cohorts.** (A) Serial intervals are typically measured from the cohort of infectors who develop symptoms at the same time. In this case, infectors will have shorter incubation periods than their infectees on average; the corresponding generation intervals will be also short because infectors with short incubation periods will transmit earlier. (B) Generation intervals for the cohort of infectors who are infected at the same time will have unbiased incubation periods.

infection-based generation interval: $E[\tau_{g,\text{inf}}] > \mathbb{E}[\tau_{g,\text{symp}}]$. Therefore, the difference between the mean serial interval and the mean infection-based generation interval is difficult to predict in general; in most cases, however, we expect the former effect to dominate, causing the mean serial interval to be longer than the mean infection-based generation interval: $\mathbb{E}[\tau_s] > E[\tau_{g,\text{inf}}]$ [3]. Earlier work on serial-interval distributions neglected dynamical biases in the incubation periods of the infectors [10, 11], which allowed them to conclude that the mean generation and serial intervals are identical. For simplicity, we will use the term "forward generation-interval" to refer to the infection-based generation-interval distribution (measured from a cohort of infectors who were infected at the same infection time, Fig. 1B), and drop the subscript inf.

Assuming that the incidence of infection is changing exponentially at a constant rate r, the forward serial-interval distribution for a cohort of infectors who developed symptoms at the same time t is expected to remain unchanged across t [3]. Then, we can focus on the forward serial-interval distribution at $t = 0$, which in turn allows us to reparameterize the incubation-period and generation-interval distributions in terms of the infection time of the infector $\alpha_1 < 0$ and of the infectee $\alpha_2 > \alpha_1$. Under this parameterization, for a given length of a serial interval τ, we can rewrite the incubation period of the infector as $-\alpha_1$; the generation interval as $\alpha_2 - \alpha_1$; and the incubation period of the infectee as $\tau - \alpha_2$. Then, the forward serial-interval distribution $f_S(\tau)$ for a cohort of infectors who developed symptoms at time $t = 0$ can be expressed in terms of three distributions (Eq. (3)): the backward incubation-period distribution of the infector $b_I(-\alpha_1)$, the forward generation-interval distribution conditional on a known value of the incubation period x, $f_{G|I}(\alpha_2 - \alpha_1| - \alpha_1)$, and the forward incubation-period distribution of the infectee $f_I(\tau - \alpha_2)$. Integrating across infection time of the infector $\alpha_1 < 0$ and of the infectee $\alpha_2 > \alpha_1$ and rewriting the backward incubation-period distribution $b_I(-\alpha_1)$ in terms of the forward distribution, we obtain [3]:

$$f_S(\tau) = \frac{1}{\phi} \int_{-\infty}^{0} \int_{\alpha_1}^{\tau} \exp(r\alpha_1) f_{G|I}(\alpha_2 - \alpha_1| - \alpha_1) f_I(-\alpha_1) f_I(\tau - \alpha_2) \, \mathrm{d}\alpha_2 \, \mathrm{d}\alpha_1, \qquad (6)$$

where ϕ is a normalization constant chosen so that $\int f_S(x) \, \mathrm{d}x = 1$. As discussed earlier, this method assumes that the incidence is changing exponentially at a constant rate r across the study period. As we show later in the results section, the exponential growth rate changes over the study period, including weeks 50 and 51 (13–26 December 2021); for illustrative purpose, we choose values of r that represent the dynamics of Delta and Omicron infections during this period and repeat the analysis across plausible ranges of r (discussed later in detail).

While the derivation of the forward serial-interval distribution Eq. (6) may be complex, its implementation is simple. The main difference between our model and previous models that neglect dynamical effects [9, 12, 13, 14] is the exponential growth term $\exp(r\alpha_1)$ and the normalization term ϕ—it is relatively straightforward to include these terms in existing models of serial intervals. [15, 16] also included this term in their analyses of serial-interval data, but only accounted for the epidemic

growth effect (and not the decay effect).

We model the forward incubation-period $f_I(\tau)$ and generation-interval $f_G(\tau)$ distributions using a bivariate lognormal distribution. The joint distribution is parameterized by log means, μ_I and μ_G, log variances, σ_I^2 and σ_G^2, and the correlation coefficient on a log scale ρ. Thus, the forward generation-interval distribution conditional on the incubation period $f_{G|I}(\tau|\tau_{i,1})$ has a log mean of $\mu_G + \sigma_G\rho(\log(\tau_{i,1}) - \mu_I)/\sigma_I$ and a log variance of $\sigma_G^2(1-\rho^2)$. For a given value of r, we first estimate the forward incubation-period distribution from the backward distribution, previously estimated by [4], using Eq. (2). We then approximate the forward incubation-period distribution with a lognormal distribution by matching the mean and standard deviation. Using this incubation-period distribution, we fit Eq. (6) to the observed serial-interval data by minimizing the negative log-likelihood. We then calculate the mean forward generation interval using Eq. (5). The 95% confidence intervals are calculated by taking the estimated variance-covariance matrix for the log-mean and -standard deviation parameters of the log normal distributions and calculating the corresponding variance-covariance for the overall mean using Taylor expansion—this method is also known as the Delta method [17]. We assume $\rho = 0.75$ throughout based on [18]—since we do not have individual-level data on infection and symptom onset times, we expect this parameter to be unidentifiable in practice. In Supplementary Material, we explore how assumptions about ρ affect inferences of the generation-interval distribution.

2.5 Estimating instantaneous reproduction numbers

We use our estimates of the generation-interval distributions to infer instantaneous reproduction numbers $\mathcal{R}(t)$ of the Delta and Omicron variant, as well as the ratio between two reproduction numbers. Estimating the instantaneous reproduction number—defined as the average number of secondary infections that a primary case will generate if epidemiological conditions remain constant [19]—requires the intrinsic generation-interval distribution $g(\tau)$:

$$\mathcal{R}(t) = \frac{i(t)}{\int_0^\infty i(t-x)g(x)\,\mathrm{d}x}, \tag{7}$$

where $i(t)$ represents incidence of infection. Here, we approximate the intrinsic generation-interval distribution with the forward generation-interval that we estimate for weeks 50 and 51 of 2021 (13–26 December)—when the epidemic is growing or decaying exponentially, we expect the forward generation-interval to be a good proxy for the intrinsic generation-interval distribution [20, 21]. Incidence of infection is approximated by shifting the smoothed case trajectories by one week to account for reporting delays. This method of approximating incidence of infection assumes a fixed delay between infection and case reporting; in practice, deconvolution is required to accurately estimate the incidence of infection [22]. Case reports are also sensitive to changes in testing behavior, and therefore our estimates of $\mathcal{R}(t)$ must be

interpreted with care. Confidence intervals are calculated by sampling parameters of the smoothed case trajectories as well as the generation-interval distributions from multivariate normal distributions and repeating the analysis 1000 times.

3 Results

Fig. 2 summarizes the epidemiological context in the Netherlands during the study period. The first known Omicron case in the Netherlands was sampled on 19 November 2021 [4], during a period when COVID-19 incidence was decreasing (Fig. 2A). As the Omicron variant continued to spread and increase in proportion (Fig. 2B), the number of COVID-19 cases started to increase (Fig. 2A). Multiplying the proportion of each variant with the number of reported COVID-19 cases further allows us to estimate the epidemiological dynamics of each (Fig. 2C). The number of COVID-19 cases caused by the Delta variant continued to decrease throughout the study period with time-varying growth rates decreasing from $r \approx -0.01$/day to $r \approx -0.09$/day by the week of January 16, 2022, and increasing back up to $r \approx -0.04$/day by the end of January, 2022. The number of COVID-19 cases caused by the Omicron variant increased rapidly but decelerated over time with time-varying growth rates decreasing from $r = 0.18$/day on the week of December 19, 2021, to $r = 0.04$/day by the end of January, 2022. These changes in growth rates coincide with the introduction of lockdown on 19 December 2021 [23] and its relaxation beginning 15 January 2022 [24, 25]. We note that the growth-rate difference between the Delta and Omicron variants decreased over time. Hereafter, we use $r = -0.05$/day for the Delta variant and $r = 0.15$/day for the Omicron variant as representative growth rates—these growth rates correspond to the mean growth rates between 1 December 2021 and 2 January 2022, during which the incubation-period data were collected. We then evaluate the growth-rate effects across $r = -0.1$/day–0.0/day for the Delta variant and $r = 0.1$/day–0.2/day for the Omicron variant as a sensitivity analysis.

Previous analysis of a cohort of individuals who developed symptoms between 1 December 2021 and 2 January 2022 found longer mean (backward) incubation period for the Delta variant than for the Omicron variant [4] (Fig. 3A). However, these measurements were done during a period when the incidence of Omicron was increasing while the increasing of Delta was decreasing (Fig. 2). Thus, dynamical bias would be expected to lead to shorter observed (backward) incubation periods in Omicron, and longer observed incubation periods in Delta. When we account for these growth-rate differences and re-estimate the forward incubation periods, we find that both variants have similar incubation-period distributions with a mean of 4.1 days (Fig. 3B); in this case, the difference between the mean backward and forward incubation periods correspond to -22% and 7% bias for the Omicron and Delta variants, respectively. Although the exact estimate of the mean forward incubation periods of both variants are sensitive to the assumed growth/decay rates, we find similar means across a plausible ranges of growth rates (Fig. 3C–D). For example, the

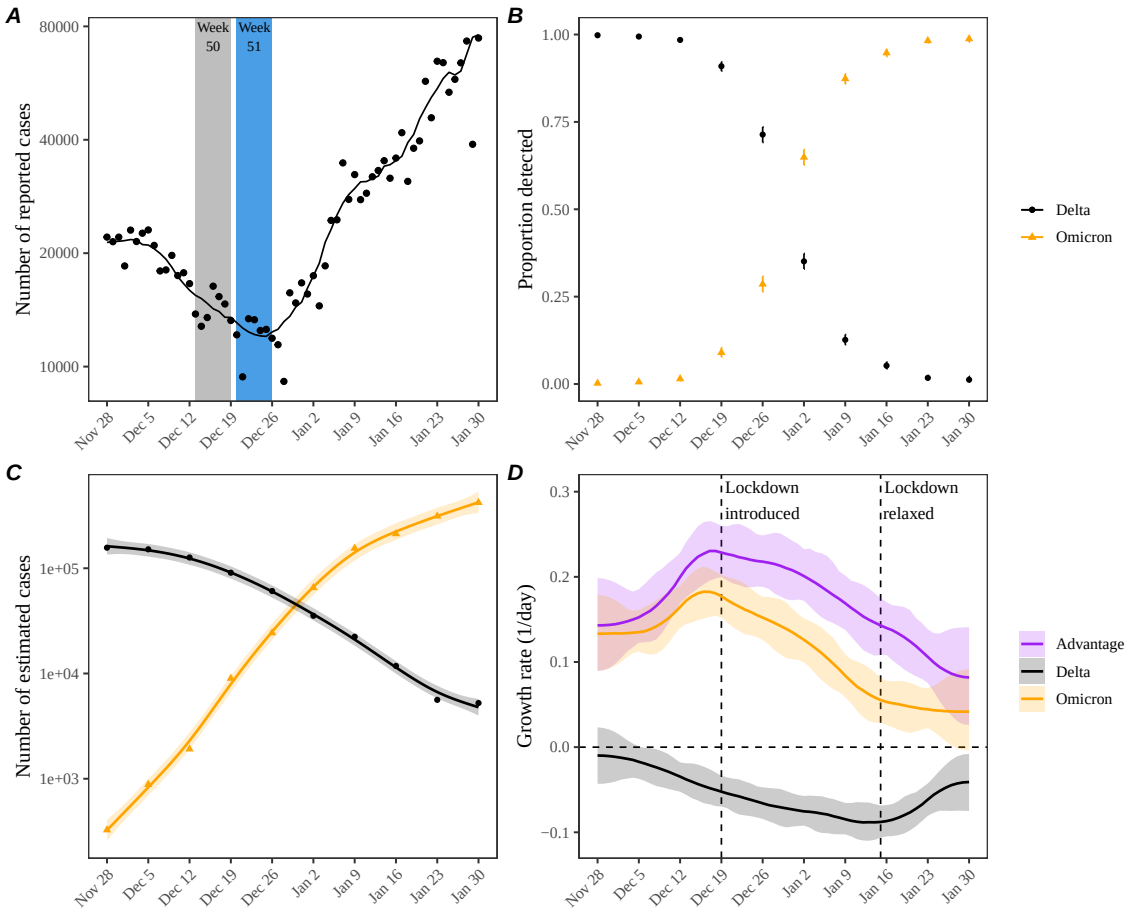

Figure 2: **Epidemic dynamics on the Delta and Omicron variants in the Netherlands between November 2021 and January 2022.** (A) Daily numbers of reported COVID-19 cases in the Netherlands (points). The solid line represents the 7-day moving average. Data are publicly available on `https://data.rivm.nl/covid-19/`. (B) Proportion of SARS-CoV-2 variants detected from the Netherlands. Data are publicly available on `https://www.rivm.nl/coronavirus-covid-19/virus/varianten`. (C) Weekly numbers of COVID-19 cases caused by the Delta (black points) and Omicron (orange triangles) variants are estimated by multiplying the weekly numbers of cases (A) with the proportion of each variant (B). Solid lines and shaded areas represent fitted lines and corresponding 95% confidence intervals using generalized additive model. (D) Estimated growth rates of the Delta (black) and Omicron variants (orange) and their growth-rate differences (purple). Lines and shaded areas represent medians and corresponding 95% confidence intervals. Growth rates are estimated by taking the derivative of the generalized additive model estimates.

mean forward incubation period of the Delta variant changes from 3.8 days (95% CI: 3.5–4.1 days) to 4.4 days (95% CI: 4.0–4.8 days) as we change the assumed values of

r from -0.1/days to 0/days (Fig. 3C), while the mean forward incubation period of the Omicron variant changes from 3.8 days (95% CI: 3.4–4.4 days) to 4.5 days (95% CI: 3.9–5.5 days) as we change the assumed values of r from 0.1/days to 0.2/days (Fig. 3D).

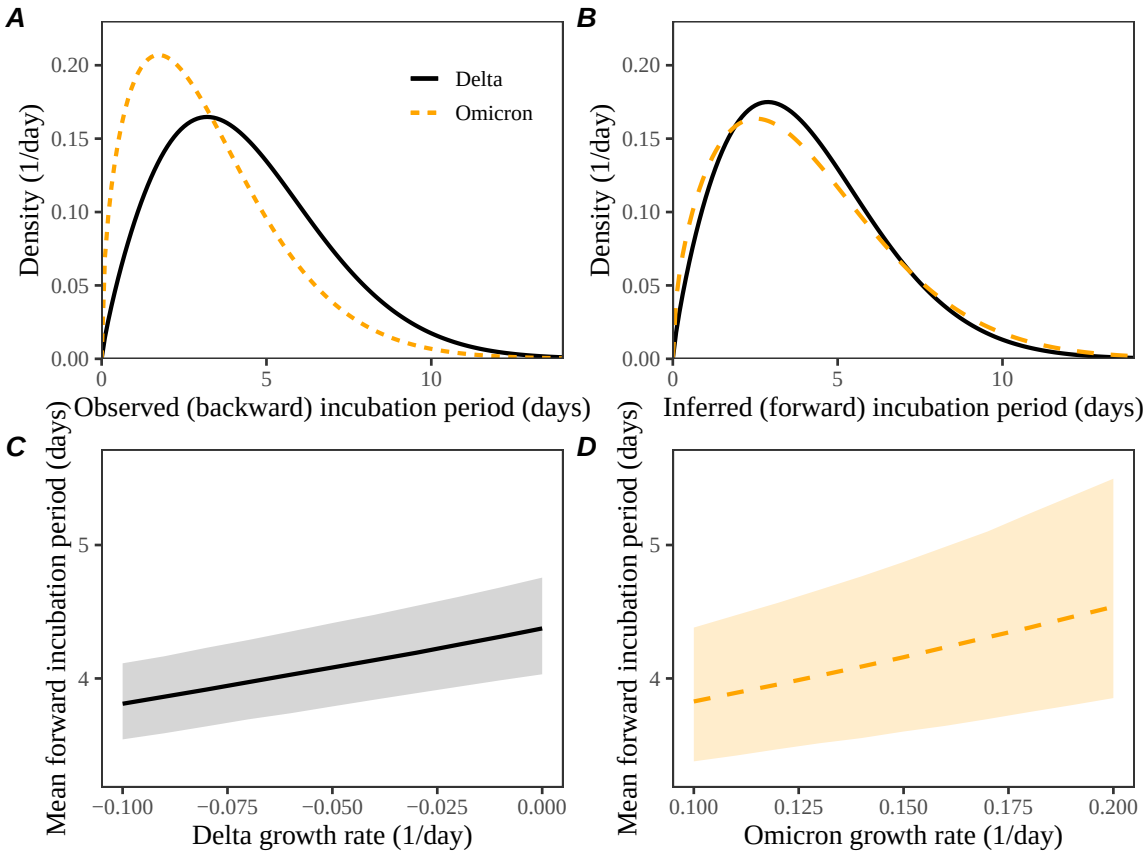

Figure 3: **Observed and corrected differences in incubation-period distributions of Delta and Omicron variants.** (A) Posterior median estimates of the observed (backward) incubation periods of the Delta (black) and Omicron (orange) variants by [4]. (B) Forward incubation-period distributions assuming $r = -0.05$/day and $r = 0.15$/day for the Delta (black) and Omicron (orange) variants, respectively. (C–D) Corrected estimates of the mean forward incubation-period for different assumptions about the growth rates of the Delta (C) and Omicron variants (D). Lines represent median estimates. Shaded regions represent the corresponding 95% confidence intervals.

Our corrected estimates of the forward incubation-period distributions further allow us to infer the forward generation-interval distributions. For illustrative purposes, we first focus on aggregated serial intervals from infectors who developed symptoms during week 50–51 (13–26 December, 2021). For within-household transmission pairs (Fig. 4A), the Omicron variant has shorter mean serial interval (3.1 days; 95% CI: 2.9–3.3 days) than that of the Delta variant (3.7 days; 95% CI: 3.5–3.8

days). When we account for growth-rate differences (assuming $r = -0.05$/day and $r = 0.15$/day for the Delta and Omicron variants, respectively), the estimated mean forward generation interval exhibits a slightly larger difference (Fig. 4B): 3.0 days (95% CI: 2.7–3.2 days) for the Omicron variant and 3.8 days (95% CI: 3.7–4.0 days) for the Delta variant. Across plausible ranges of assumptions about the growth rates of the Delta and Omicron variants, we estimate robust differences in their mean generation intervals (Fig. 4C–D). Assuming lower values of the correlation ρ between the incubation period and generation intervals leads to larger differences in the mean generation intervals of the Delta and Omicron variants (Supplementary Figure S1). In particular, the generation-interval estimates of the Omicron variant are more sensitive to the assumed values of ρ due to faster changes in incidence of infection—for example, changing ρ from 0.85 to 0.5 changes the mean generation-interval estimates for the Omicron variant from 3.1 days (95% CI: 2.8–3.3 days) to 2.7 days (95% CI: 2.5–2.9 days).

Similar pictures arise for between-household transmission pairs, but the differences in mean serial intervals are unclear (Fig. 4E): 3.0 days (95% CI: 2.7–3.3 days) for the Omicron variant and 3.3 days (95% CI: 3.0 days–3.6 days) for the Delta variant. Consistent with the original study, which also reported shorter mean serial intervals for between-household pairs [4], we estimate shorter mean generation intervals for between-household Delta pairs. While the difference in mean generation intervals is larger, there is greater uncertainty in their mean estimates (Fig. 4F): 2.9 days (95% CI: 2.5–3.3 days) for the Omicron variant and 3.5 days (95% CI: 3.2–3.8 days) for the Delta variant. Once again, these patterns are robust across plausible ranges of assumptions about the growth rates of the Delta and Omicron variants (Fig. 4G–H).

In Supplementary Figure S2, we present generation-interval estimates that are further stratified by the week of infectors' symptom onset (13–19 December 2021 and 20–26 December 2021). While we generally estimate shorter mean generation intervals for the Omicron variant, but the differences are unclear across all stratification, except for within-household transmission pairs during week 50 (13–19 December 2021). We also estimate a reduction in the mean forward generation intervals from week 50 (13–19 December 2021) to week 51 (20–26 December 2021), especially for the Delta variant.

Accounting for differences in the generation-interval distributions, we estimate that the instantaneous reproduction number of the Omicron variant decreased from 1.73 (95% CI: 1.59–1.89) to 1.14 (95% CI: 1.00–1.32) between December 12, 2021, and January 23, 2022(Fig. 5A). On the other hand, the instantaneous reproduction number of the Delta variant decreased from 0.90 (95% CI: 0.83–0.97) to 0.69 (95% CI: 0.65–0.75) between December 5, 2021, and January 9, 2022, and increased back up to 0.83 (95% CI: 0.73–0.94) by January 23, 2022 (Fig. 5A). We estimate the reproduction advantage (i.e., the ratio between the instantaneous reproduction numbers of the Omicron and Delta variants) stayed roughly constant at around 2.10 (95% CI: 1.90–2.33) between December 12–26, 2021, and slowly decreased to 1.38

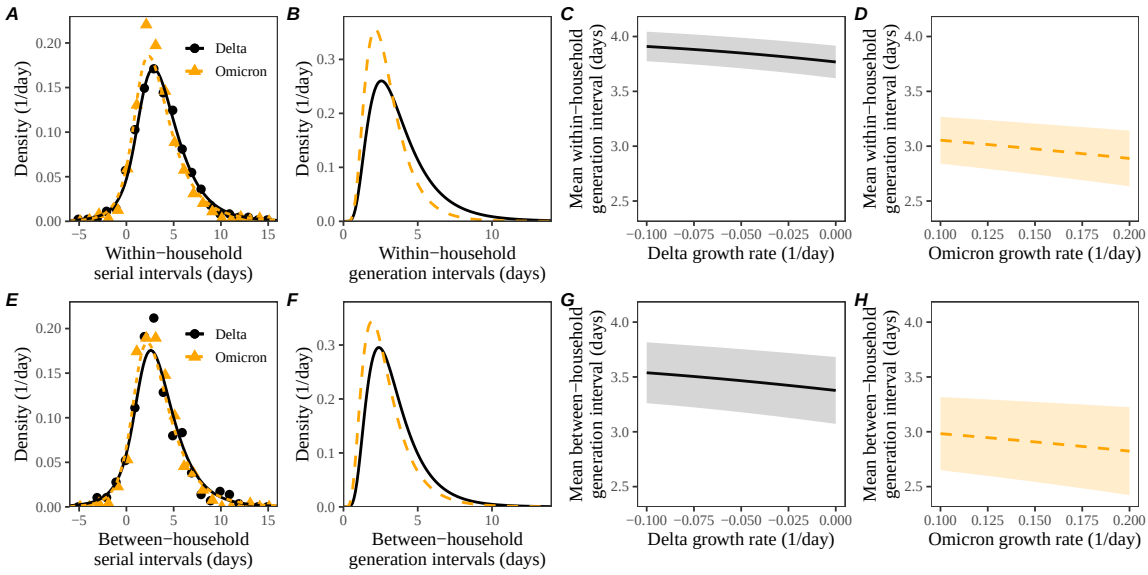

Figure 4: **Estimated forward generation-interval distributions of Delta and Omicron variants.** (A, E) Observed and fitted forward serial-interval distributions for within-household (A) and between-household (E) transmission pairs in the Netherlands for the Delta (black) and Omicron (orange) variants [4]. Serial intervals are calculated for infectors who developed symptoms on weeks 50 and 51 (13–26 December, 2021). Points represent the observed data. Lines represent the fitted lines assuming $r = -0.05$/day for the Delta variant and $r = 0.15$/day for the Omicron variant. (B, F) Estimated forward generation-interval distributions for within-household (B) and between-household (F) transmission pairs in the Netherlands. (C, D, G, H) Sensitivity of the mean forward generation-interval estimates to assumed growth rates of the Delta (C, G) and Omicron variants (G, H) for within-household (C, D) and between-household (G, H) transmission pairs. Lines represent maximum likelihood estimates. Shaded regions represent the corresponding 95% confidence intervals.

(95% CI: 1.15–1.65). However, if we neglect differences in the generation-interval distributions and solely rely on the generation-interval-distribution estimate for the Delta variant, we over-estimate the reproduction number of the Omicron variant and therefore the reproduction advantage (Fig. 5B). In this case, the reproduction advantage decreases from 2.38 (95% CI: 2.13–2.67) to 1.43 (95% CI: 1.17–1.75), corresponding to roughly 4–13% bias. Using between-household generation intervals also gives similar conclusions about changes and biases in the reproduction number estimates (Supplementary Figure S3).

In both cases, the decrease in the reproduction advantage coincides with the decrease in the reproduction number of the Omicron variant, implying that epidemiological changes driving the dynamic had larger effects on the transmission of the Omicron variant than on the transmission of Delta variant; a larger reduction in the

reproduction number of the Omicron variant also caused its growth rate to decrease faster, causing changes in the observed growth-rate difference (Fig. 2D).

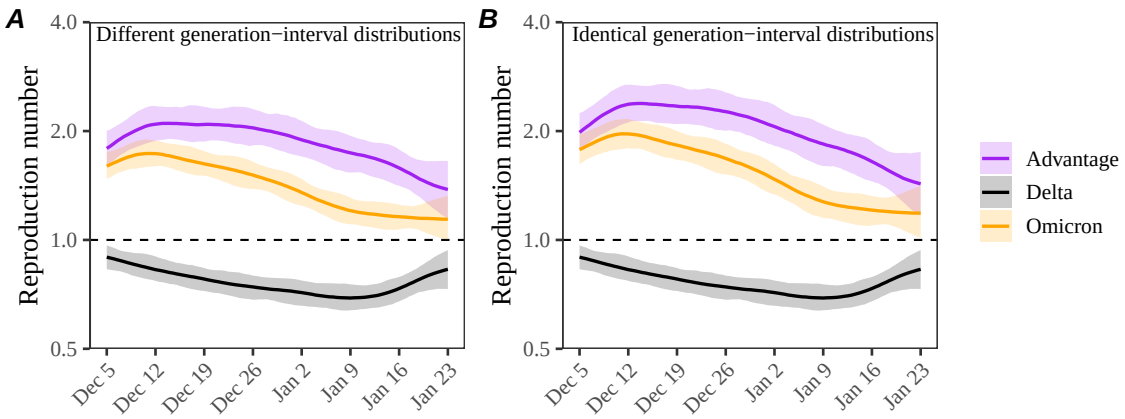

Figure 5: **Estimated instantaneous reproduction number advantages of the Omicron variant.** (A) Estimated instantaneous reproduction numbers and their ratios over time while accounting for differences in the generation-interval distributions. (B) Estimated instantaneous reproduction numbers and their ratios over time while assuming identical generation-interval distributions. The instantaneous reproduction number of each variant is estimated using the renewal equation by shifting the smoothed case curves by one week (Fig. 2C). The intrinsic generation-interval distribution is approximated by the maximum likelihood estimates of the forward generation-interval distributions for within-household transmission pairs based on $r = -0.05$ for the Delta variant (black) and $r = 0.15$ for the Omicron variant (orange). Purple lines represent the ratio between the effective reproduction numbers of the Delta and Omicron variants. Lines and shaded regions represent medians and corresponding 95% confidence intervals.

4 Discussion

We compare estimates of the forward incubation-period and generation-interval distributions of the Delta and Omicron variants from the Netherlands in late 2021 and early 2022. The original analysis detailing the data set previously reported a shorter mean incubation period and serial interval for the Omicron variant [4]. Accounting for differences in epidemic growth rates, however, we find similar incubation-period distributions for both variants but a shorter (0.3–0.8 days) mean generation interval for the Omicron variant relative to that of the Delta variant. Finally, we estimate that the transmission advantage of the Omicron variant decreased from 2.1-fold to 1.4-fold between early December and late January. Improving generation-interval estimates by taking dynamical effects into account may improve understanding of epidemic dynamics and control measures.

The generation-interval distribution describes changes in the individual-level transmission dynamics over the course of infection and therefore provides crucial information for epidemic control. A few studies have estimated the generation-interval distributions of SARS-CoV-2 infections from serial-interval data, but most of them neglect the effects of epidemic growth rates [9, 12, 13, 14]—these practices can be largely attributed to historical work that concluded that serial and generation intervals have the same means based on the assumption that infectors and infectees have identical incubation-period distributions [10, 11, 26]. We build on newer work [3], which demonstrated theoretically that forward serial-interval distributions depend on epidemic growth rates, and further confirm that estimates of the forward generation-interval distributions are indeed sensitive to epidemic growth rates. These effects are also pertinent to epidemiological inferences of past events from a cohort of infected individuals who experienced a later event at the same time—this includes inferences of other delay distributions, such as incubation-period distributions, as well as viral load trajectories [27]. Our sensitivity analysis also shows that the assumptions about the correlation between incubation periods and generation intervals can also have important effects on the estimates of the generation-interval distributions (Supplementary Figure S1).

This study presents a simple method for accounting for dynamical biases in inferring incubation-period distributions based on epidemic growth rates. In practice, it is easier to measure the backward incubation-period distribution in practice because we can directly observe symptom onset. Therefore, the observed incubatiod-period distributions are generally expected to be biased, and similar kinds of corrections will be necessary to accurately estimate the incubatiod-period distribution. We note that making these kinds of corrections will also depend on data availability, model complexity, and other epidemiological variables affecting incubation periods, such as vaccine statuses. Accounting for different sources of biases is critical to accurately estimating incubation-period distributions (and other epidemiological distributions alike) but will necessarily increase uncertainties in the estimates. On the other hand, it is still possible to characterize the forward incubation-period distributions without making growth-rate-based corrections through careful cohorting based on infection time when detailed information about infection time is available.

A few studies have suggested the the incubation period of the Omicron variant may be shorter than that of the Delta variant. The median estimates of the Omicron incubation period typically range between 3–4 days, consistent with earlier findings of [4]. However, these data were collected when the number of Omicron infections was growing rapidly [28, 29], suggesting that they may have been subject to similar biases. On the other hand, incubation-period estimates based on individuals who were exposed from the same event are likely more reliable (because they look forward in time): [30] estimated the median incubation period of the Omicron variant to be 3 days among those who attended the same holiday party ($n = 117$) on 26 November 2021 in Norway. However, we cannot rule out the possibility that some of these attendees were infected prior to the party given that some individuals had COVID-

like symptoms prior to the party with at least 96 of the attendees sharing offices; neglecting these factors can lead to underestimation of the mean incubation period. Systematic comparisons of data collection methods and epidemiological contexts are needed to properly assess the differences in incubation period distributions of the Delta and Omicron variants.

A few studies have estimated that the Omicron variant has shorter transmission intervals than the Delta variant [2, 31, 29], but there has been a lack of direct generation-interval estimates. [32, 33] tried to estimate the generation-interval distributions of the Omicron variant but they both relied on population-level epidemic dynamics (rather than individual-level transmission data). Although we estimate a shorter mean generation interval for the Omicron variant, we find the generation-interval distribution of the Omicron and Delta variants have similar modes (around 2.5 days), implying that the realized transmissibility of the Omicron variant decays faster. We tentatively hypothesize that these differences may be primarily driven by the network effect [21, 14]: a higher reproduction numbers of the Omicron variant leads to faster susceptible depletion among close contacts, which in turn prevents long generation intervals from generating infections. While the network effect is expected to be strongest among household contacts, it is also applicable to other forms of contact structures that involve repeated contacts between the same group of individuals (because only the first infectious contact results in infection). The network effect may also explain a decrease in the mean generation interval between week 50 and 51 (13–26 December 2021), especially among household transmission pairs, as a higher proportion of individuals within households would have been infected with either the Delta or Omicron variants. Shorter generation-interval estimates for between-household contacts may be attributable to behavioral effects: individuals who have symptoms or tested positive may be more likely to stay home, preventing long between-household transmission. Other factors, such as more stringent intervention measures against the Omicron variant [4] and faster within-host clearance of the Omicron variant [34], also likely contributed to shortening of generation intervals.

While our study indicates that the Omicron variant has a shorter mean realized generation interval than that of the Delta variant, it is still uncertain how infectiousness profiles differ intrinsically between Omicron and Delta. In particular, similarities in the incubation-period distributions of the Delta and Omicron variants suggest that the differences in their true infectiousness profile may be smaller than the estimated differences in their realized generation-interval distributions. In addition, the "intrinsic" generation intervals of both Omicron and Delta variants are likely longer than what we estimate given existing levels of interventions, including vaccination, and pandemic awareness—estimating intrinsic (or "unmitigated") generation-interval distributions of SARS-CoV-2 variants is expected to be a difficult problem as it requires data from times when awareness levels were low [18]. Nonetheless, our estimates of the realized generation-interval distributions better describe current epidemic dynamics, implicitly accounting for intervention and behavioral effects, and can therefore be expected to improve estimates of effective

reproduction numbers.

Our study also has important implications for estimating transmission advantages of new SARS-CoV-2 variants. In the example we consider, neglecting differences in the generation-interval distributions leads to $\approx 10\%$ bias in the estimates of the reproduction advantage (i.e., the ratio between the reproduction numbers of the Omicron and Delta variants). More generally, the bias in inferring the reproduction advantage an emerging variant is expected to be sensitive to the assumed generation-interval distribution of the resident variant. For example, [35] estimated a much higher reproduction advantage of the Omicron variant (> 4 fold) compared to the Delta variant in South Africa but also assumed a longer mean generation interval for the Delta and Omicron variants (6.4 vs 5.2 days, respectively). With our generation-interval estimates, we estimate that the reproduction advantage of 2.6 for the Omicron variant assuming $r = -0.06$ and $r = 0.26$ for the Delta and Omicron variants, respectively—these growth rates were chosen to match the 4-fold reproduction advantage with the estimated growth-rate differences of 0.32/day for the Gauteng province, South Africa [35].

We considered two ways of measuring transmission advantages: growth-rate differences and reproduction advantage. Characterizing new variants in terms of their reproduction advantage is useful because it is directly related to the amount of increased transmissibility and immune evasion [35]. On the other hand, the growth-rate difference is easier to estimate in real time is also more directly relevant to short-term dynamics. For example, when two strains have the same $\mathcal{R}$, the one with shorter generation intervals will grow faster and replace the other strain—this transmission advantage is captured by the growth-rate difference, but not by the ratio of reproduction numbers of two strains. Therefore, we suggest using growth-rate differences and reproduction advantage as complementary measures for understanding the dynamics of emerging SARS-CoV-2 variants.

We primarily rely on case data to understand epidemic patterns of the Delta and Omicron variants. In doing so, we implicitly assume that the delay between infection and reports is fixed. However, changes in case trajectories are sensitive to testing patterns and therefore may not accurately reflect patterns of infections. While this limitation does not affect our generation-interval estimates, our inferences of the transmission advantages of the Omicron variant should be interpreted with care.

Monitoring changes in key epidemiological parameters is critical to understanding the evolution of SARS-CoV-2 and predicting its future dynamics [36]. Our study synthesizes a previously developed theoretical framework on serial- and generation-interval distributions and presents methodological advances in monitoring epidemiological parameters. Similar efforts will be critical to improve estimates of the infectiousness profiles of future SARS-CoV-2 variants, especially among asymptomatically infected individuals [37].

Supplementary Materials

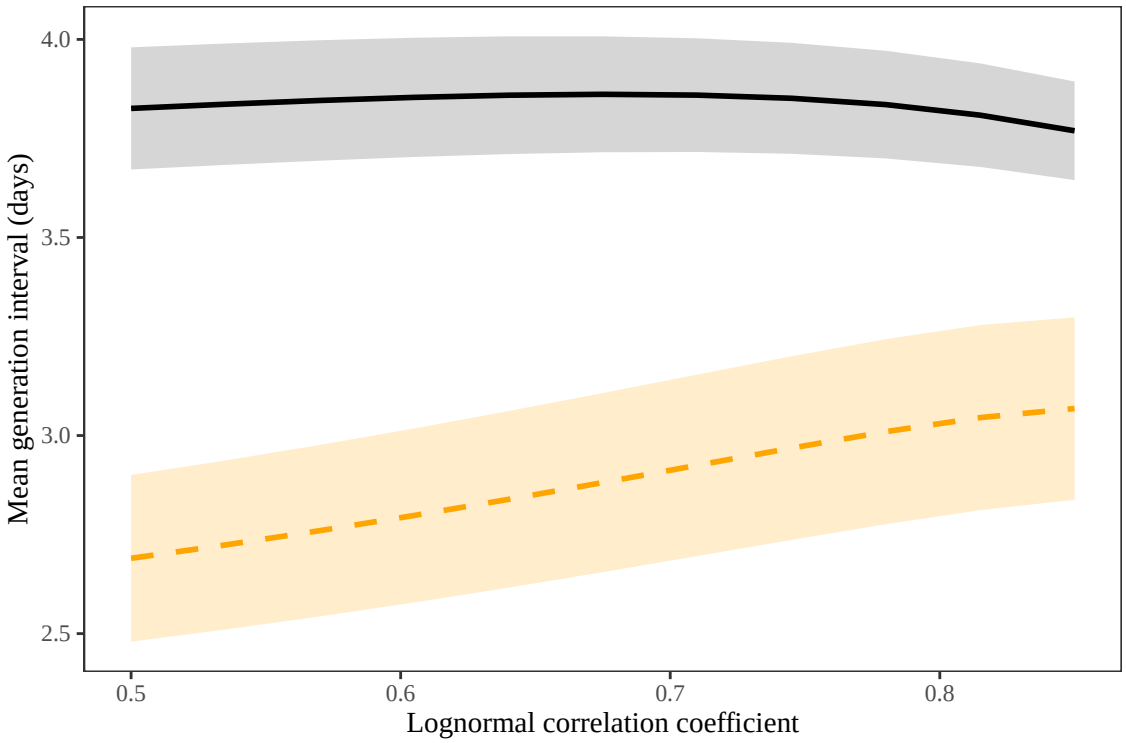

Figure S1: **Sensitivity of the estimates of the mean generation interval to the assumed values of the correlation coefficient of the lognormal distribution.** Lines and shaded regions represent maximum likelihood estimates and the corresponding 95% confidence intervals for the Delta (black, solid lines) and Omicron variants (orange, dashed lines). For illustrative purposes we use within-household serial-interval data from the cohort of infectors who developed symptoms during weeks 50 (13–19 December) and 51 (20–26 December) of 2021.

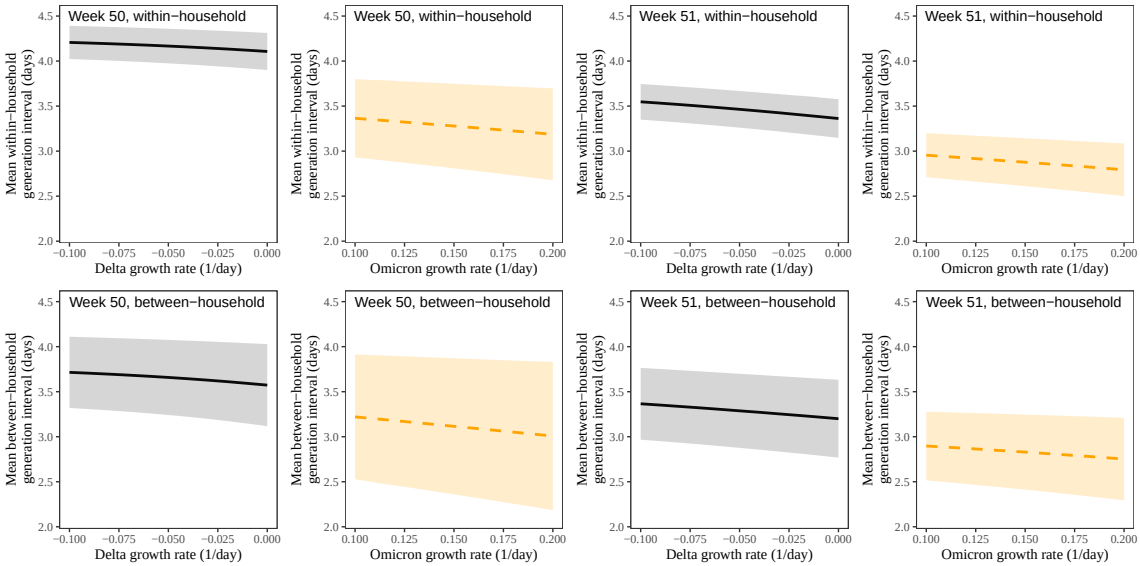

Figure S2: **Estimated mean forward generation intervals of Delta and Omicron variants across different stratifications.** Sensitivity of the mean forward generation-interval estimates to assumed growth rates of the Delta and Omicron variants stratified by the types of transmission (within- vs between-household transmission) and the week of infectors' symptom onset (week 50, 13–19 December 2021, vs week 51, 20–26 December 2021,). Lines represent maximum likelihood estimates. Shaded regions represent the corresponding 95% confidence intervals.

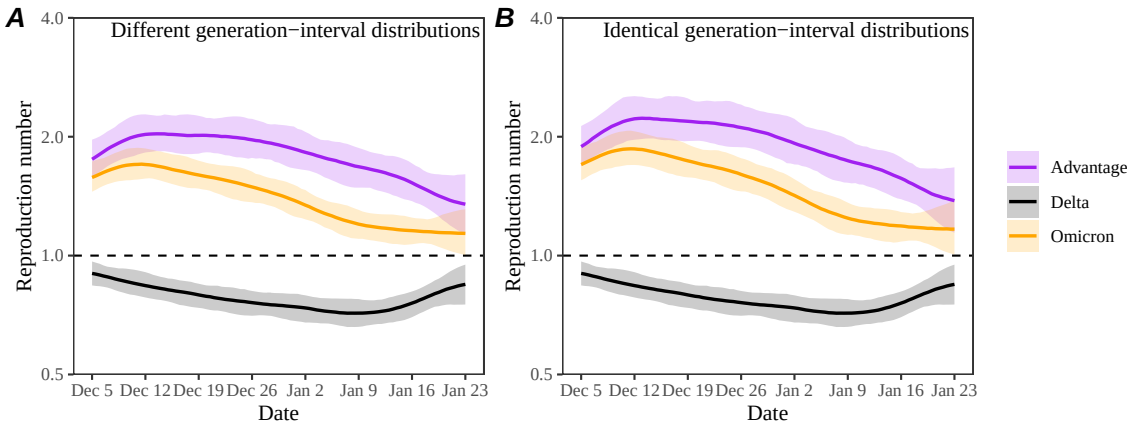

Figure S3: **Estimated time-varying reproduction number advantages of the Omicron variant using between-household generation-interval distributions.** (A) Estimated instantaneous reproduction numbers and their ratios over time while accounting for differences in the generation-interval distributions. (B) Estimated instantaneous reproduction numbers and their ratios over time while assuming identical generation-interval distributions. The instantaneous reproduction number of each variant is estimated using the renewal equation by shifting the smoothed case curves by one week (Fig. 2C). The intrinsic generation-interval distribution is approximated by the maximum likelihood estimates of the forward generation-interval distributions for between-household transmission pairs based on $r = -0.05$ for the Delta variant (black) and $r = 0.15$ for the Omicron variant (orange). Purple lines represent the ratio between the effective reproduction numbers of the Delta and Omicron variants. Lines and shaded regions represent medians and corresponding 95% confidence intervals.

References

[1] Sang Woo Park, Benjamin M Bolker, Sebastian Funk, C Jessica E Metcalf, Joshua S Weitz, Bryan T Grenfell, and Jonathan Dushoff. Roles of generation-interval distributions in shaping relative epidemic strength, speed, and control of new SARS-CoV-2 variants. *medRxiv*, 2021.

[2] Sam Abbott, Katharine Sherratt, Moritz Gerstung, and Sebastian Funk. Estimation of the test to test distribution as a proxy for generation interval distribution for the Omicron variant in England. *medRxiv*, 2022.

[3] Sang Woo Park, Kaiyuan Sun, David Champredon, Michael Li, Benjamin M Bolker, David JD Earn, Joshua S Weitz, Bryan T Grenfell, and Jonathan Dushoff. Forward-looking serial intervals correctly link epidemic growth to reproduction numbers. *Proceedings of the National Academy of Sciences*, 118(2), 2021.

[4] Jantien A Backer, Dirk Eggink, Stijn P Andeweg, Irene K Veldhuijzen, Noortje van Maarseveen, Klaas Vermaas, Boris Vlaemynck, Raf Schepers, Susan van den Hof, Chantal BEM Reusken, and Jacco Wallinga. Shorter serial intervals in SARS-CoV-2 cases with Omicron BA.1 variant compared with Delta variant, the Netherlands, 13 to 26 December 2021. *Eurosurveillance*, 27(6):2200042, 2022.

[5] Simon N Wood. mgcv: GAMs and generalized ridge regression for R. *R News*, 1(2):20–25, 2001.

[6] Jay M Ver Hoef and Peter L Boveng. Quasi-poisson vs. negative binomial regression: how should we model overdispersed count data? *Ecology*, 88(11):2766–2772, 2007.

[7] Jantien A Backer, Don Klinkenberg, and Jacco Wallinga. Incubation period of 2019 novel coronavirus (2019-nCoV) infections among travellers from Wuhan, China, 20–28 January 2020. *Eurosurveillance*, 25(5):2000062, 2020.

[8] Sang Woo Park, Benjamin M Bolker, David Champredon, David JD Earn, Michael Li, Joshua S Weitz, Bryan T Grenfell, and Jonathan Dushoff. Reconciling early-outbreak estimates of the basic reproductive number and its uncertainty: framework and applications to the novel coronavirus (SARS-CoV-2) outbreak. *Journal of the Royal Society Interface*, 17(168):20200144, 2020.

[9] Tapiwa Ganyani, Cecile Kremer, Dongxuan Chen, Andrea Torneri, Christel Faes, Jacco Wallinga, and Niel Hens. Estimating the generation interval for coronavirus disease (COVID-19) based on symptom onset data, March 2020. *Eurosurveillance*, 25(17):2000257, 2020.

[10] Åke Svensson. A note on generation times in epidemic models. *Mathematical biosciences*, 208(1):300–311, 2007.

[11] Tom Britton and Gianpaolo Scalia Tomba. Estimation in emerging epidemics: biases and remedies. *Journal of the Royal Society Interface*, 16(150):20180670, 2019.

[12] Xi He, Eric HY Lau, Peng Wu, Xilong Deng, Jian Wang, Xinxin Hao, Yiu Chung Lau, Jessica Y Wong, Yujuan Guan, Xinghua Tan, et al. Temporal dynamics in viral shedding and transmissibility of COVID-19. *Nature medicine*, 26(5):672–675, 2020.

[13] Shi Zhao, Biao Tang, Salihu S Musa, Shujuan Ma, Jiayue Zhang, Minyan Zeng, Qingping Yun, Wei Guo, Yixiang Zheng, Zuyao Yang, et al. Estimating the generation interval and inferring the latent period of COVID-19 from the contact tracing data. *Epidemics*, 36:100482, 2021.

[14] William S Hart, Elizabeth Miller, Nick J Andrews, Pauline Waight, Philip K Maini, Sebastian Funk, and Robin N Thompson. Generation time of the alpha and delta SARS-CoV-2 variants: an epidemiological analysis. *The Lancet Infectious Diseases*, 2022.

[15] Luca Ferretti, Chris Wymant, Michelle Kendall, Lele Zhao, Anel Nurtay, Lucie Abeler-Dörner, Michael Parker, David Bonsall, and Christophe Fraser. Quantifying SARS-CoV-2 transmission suggests epidemic control with digital contact tracing. *Science*, 368(6491):eabb6936, 2020.

[16] Luca Ferretti, Alice Ledda, Chris Wymant, Lele Zhao, Virginia Ledda, Lucie Abeler-Dörner, Michelle Kendall, Anel Nurtay, Hao-Yuan Cheng, Ta-Chou Ng, et al. The timing of COVID-19 transmission. *medRxiv*, 2020.

[17] Gary W Oehlert. A note on the Delta method. *The American Statistician*, 46(1):27–29, 1992.

[18] Ron Sender, Yinon M Bar-On, Sang Woo Park, Elad Noor, Jonathan Dushoffd, and Ron Milo. The unmitigated profile of COVID-19 infectiousness. *medRxiv*, 2021.

[19] Christophe Fraser. Estimating individual and household reproduction numbers in an emerging epidemic. *PloS one*, 2(8):e758, 2007.

[20] David Champredon and Jonathan Dushoff. Intrinsic and realized generation intervals in infectious-disease transmission. *Proceedings of the Royal Society B: Biological Sciences*, 282(1821):20152026, 2015.

[21] Sang Woo Park, David Champredon, and Jonathan Dushoff. Inferring generation-interval distributions from contact-tracing data. *Journal of the Royal Society Interface*, 17(167):20190719, 2020.

[22] Edward Goldstein, Jonathan Dushoff, Junling Ma, Joshua B Plotkin, David JD Earn, and Marc Lipsitch. Reconstructing influenza incidence by deconvolution of daily mortality time series. *Proceedings of the National Academy of Sciences*, 106(51):21825–21829, 2009.

[23] Government of the Netherlands. Slowing the spread of the Omicron variant: lockdown in the Netherlands. 2021. `https://www.government.nl/latest/news/2021/12/18/slowing-the-spread-of-the-omicron-variant-lockdown-in-the-netherlands`.

[24] Government of the Netherlands. Shops, gyms and hairdressers to reopen on Saturday 15 January. 2021. `https://www.government.nl/topics/coronavirus-covid-19/news/2022/01/14/shops-gyms-and-hairdressers-to-reopen-on-saturday-15-january`.

[25] Government of the Netherlands. Nearly all locations can be open until 22:00. 2021. `https://www.government.nl/topics/coronavirus-covid-19/news/2022/01/25/press-conference-25-january-2022`.

[26] Sonja Lehtinen, Peter Ashcroft, and Sebastian Bonhoeffer. On the relationship between serial interval, infectiousness profile and generation time. *Journal of the Royal Society Interface*, 18(174):20200756, 2021.

[27] James A Hay, Lee Kennedy-Shaffer, Sanjat Kanjilal, Niall J Lennon, Stacey B Gabriel, Marc Lipsitch, and Michael J Mina. Estimating epidemiologic dynamics from cross-sectional viral load distributions. *Science*, 373(6552):eabh0635, 2021.

[28] Lauren Jansen, Bryan Tegomoh, Kate Lange, Kimberly Showalter, Jon Figliomeni, Baha Abdalhamid, Peter C Iwen, Joseph Fauver, Bryan Buss, and Matthew Donahue. Investigation of a Sars-Cov-2 B.1.1.529 (Omicron) variant cluster——Nebraska, November–December 2021. *Morbidity and Mortality Weekly Report*, 70(5152):1782, 2021.

[29] Jin Su Song, Jihee Lee, Miyoung Kim, Hyeong Seop Jeong, Moon Su Kim, Seong Gon Kim, Han Na Yoo, Ji Joo Lee, Hye Young Lee, Sang-Eun Lee, et al. Serial intervals and household transmission of SARS-CoV-2 Omicron variant, South Korea, 2021. *Emerging Infectious Diseases*, 28(3):756, 2022.

[30] Lin T Brandal, Emily MacDonald, Lamprini Veneti, Tine Ravlo, Heidi Lange, Umaer Naseer, Siri Feruglio, Karoline Bragstad, Olav Hungnes, Liz E Ødeskaug, et al. Outbreak caused by the SARS-CoV-2 Omicron variant in Norway, November to December 2021. *Eurosurveillance*, 26(50):2101147, 2021.

[31] Cécile Kremer, Toon Braeye, Kristiaan Proesmans, Emmanuel André, Andrea Torneri, and Niel Hens. Observed serial intervals of SARS-CoV-2 for the Omicron and Delta variants in Belgium based on contact tracing data, 19 November to 31 December 2021. *medRxiv*, 2022.

[32] Kimihito Ito, Chayada Piantham, and Hiroshi Nishiura. Estimating relative generation times and relative reproduction numbers of Omicron BA.1 and BA.2 with respect to Delta in Denmark. *medRxiv*, 2022.

[33] Alex Selby. Estimating generation time of Omicron. 2022.

[34] James A Hay, Stephen M Kissler, Joseph R Fauver, Christina Mack, Caroline G Tai, Radhika M Samant, Sarah Connelly, Deverick J Anderson, Gaurav Khullar, Matthew MacKay, et al. Viral dynamics and duration of PCR positivity of the SARS-CoV-2 Omicron variant. *medRxiv*, 2022.

[35] Carl AB Pearson, Sheetal P Silal, Michael WZ Li, Jonathan Dushoff, Benjamin M Bolker, Sam Abbott, Cari van Schalkwyk, Nicholas G Davies, Rosanna C Barnard, W John Edmunds, et al. Bounding the levels of transmissibility & immune evasion of the Omicron variant in South Africa. *MedRxiv*, 2021.

[36] Moritz UG Kraemer, Oliver G Pybus, Christophe Fraser, Simon Cauchemez, Andrew Rambaut, and Benjamin J Cowling. Monitoring key epidemiological parameters of SARS-CoV-2 transmission. *Nature medicine*, 27(11):1854–1855, 2021.

[37] Sang Woo Park, Daniel M Cornforth, Jonathan Dushoff, and Joshua S Weitz. The time scale of asymptomatic transmission affects estimates of epidemic potential in the COVID-19 outbreak. *Epidemics*, 31:100392, 2020.